Inorganica Chimica Acta 362 (2009) 3314–3324

Contents lists available at ScienceDirect

Inorganica Chimica Acta

journal homepage: www.elsevier.com/locate/ica

(Pyrazolylmethyl)pyridine platinum(II) and gold(III) complexes: Synthesis, structures and evaluation as anticancer agents

Tebogo V. Segapelo [a], Ilia A. Guzei [b], Lara C. Spencer [b], Werner E Van Zyl [a,1], James Darkwa [a,*]

[a] Department of Chemistry, University of Johannesburg, Auckland Park Kingsway Campus, P.O. Box 524, Johannesburg 2006, South Africa
[b] Department of Chemistry, University of Wisconsin-Madison, 1101 University Avenue, Madison, WI 53706, USA

ARTICLE INFO

Article history:
Received 4 September 2008
Received in revised form 18 February 2009
Accepted 28 February 2009
Available online 9 March 2009

Keywords:
(Pyrazol-1-ylmethyl)pyridine ligands
Platinum complexes
Gold complexes
C–H activation
Antitumor activity

ABSTRACT

Reactions of 2-(3,5-dimethylpyrazol-1-ylmethyl)pyridine (**L1**), 2-(3,5-diphenylpyrazol-1-ylmethyl)pyridine (**L2**), 2-(3,5-di-*tert*-butylpyrazol-1-ylmethyl)pyridine (**L3**) and 2-(3-*p*-tolylpyrazol-1-ylmethyl)pyridine (**L4**) with $K_2[PtCl_4]$ in a mixture of ethanol and water formed the dichloro platinum complexes $[PtCl_2(\mathbf{L1})]$ (**1**), $[PtCl_2(\mathbf{L2})]$ (**2**), $[PtCl_2(\mathbf{L3})]$ (**3**) and $[PtCl_2(\mathbf{L4})]$ (**4**). Complex **1,** $[PtCl_2(\mathbf{L1})]$, could also be prepared in a mixture of acetone and water. Performing the reactions of **L2** and **L3** in a mixture of acetone and water, however, led to C–H activation of acetone under mild conditions to form the neutral acetonyl complexes $[Pt(CH_2COCH_3)Cl(\mathbf{L2})]$ (**2a**) and $[Pt(CH_2COCH_3)Cl(\mathbf{L3})]$ (**3a**). The same ligands reacted with $HAuCl_4 \cdot 4H_2O$ in a mixture of ethanol and water to form the gold salts $[AuCl_2(\mathbf{L1})][AuCl_4]$ (**5**) $[AuCl_2(\mathbf{L2})][Cl]$ (**6**) $[AuCl_2(\mathbf{L3})][Cl]$ (**7**) and $[AuCl_2(\mathbf{L4})][AuCl_4]$ (**8**); however, with the pyrazolyl unit in the *para* position of the pyridinyl ring in 4-(3,5-dimethylpyrazol-1-ylmethyl)pyridine (**L5**), 4-(3,5-diphenylpyrazol-1-ylmethyl)pyridine (**L6**) neutral gold complexes $[AuCl_3(\mathbf{L5})]$ (**9**) and $[AuCl_2(\mathbf{L6})]$ (**10**) were formed; signifying the role the position of the pyrazolyl group plays in product formation in the gold reactions. X-ray crystallographic structural determination of **L6**, **2**, **3** **3a**, **8** and **10** were very important in confirming the structures of these compounds; particularly for **3a** and **8** where the presence of the acetonyl group confirmed C–H activation and for **8** where the counter ion is $AuCl_4^-$. Cytotoxicity studies of **L2**, **L4** and complexes **1**–**10** against HeLa cells showed the Au complexes were much less active than the Pt complexes.

1. Introduction

Extensive study of metals in medicine is largely due to the approval of cisplatin as a cancer drug more than three decades ago [1]. Although it is still one of the most widely used drugs in the world, the impetus to find new drugs stems from drug resistance [2–4] and severe side effects associated with the use of cisplatin [5,6]. It has been suggested that the reaction of cisplatin with some kidney enzymes' sulfhydryl groups is responsible for the drug's most severe side effects [7,8]. Over the years considerable amount of interest has focused on the use of pyridine platinum(II) complexes as mimics of cisplatin [9–13]. These studies have shown that the use of planar ligands, such as the substituted pyridines (**I**–**III**) in platinum(II) complexes, can reduce the rate of deactivation by sulfhydryl groups without interfering with DNA binding, considered to be the mode of action of cisplatin [11,12].

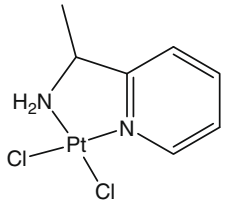

R = H (**I**), Me (**II**)

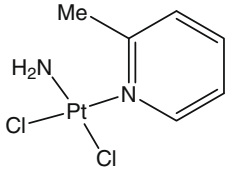

(**III**)

Several non-platinum metal complexes have also been studied as potential anticancer agents [13]. The rationale for these studies is that metal centers other than platinum might produce improved anticancer activity *in vitro* and *in vivo*. Gold(III) is one such metal ion which typically adopts a four-coordinate, square-planar geometry and is therefore expected to mimic the structural and electronic properties of platinum(II). Recent studies have shown that several gold(III) complexes are highly cytotoxic against different tumor cells [14–16], including some which are active even against the cisplatin-resistant cell lines [17–20]. Unfortunately, the use of gold(III)

* Corresponding author.
E-mail address: jdarkwa@uj.ac.za (J. Darkwa).
[1] Present address: School of Chemistry, University of KwaZulu Natal, Westville Campus, Private Bag X54001, Durban, South Africa.

0020-1693/$ - see front matter © 2009 Elsevier B.V. All rights reserved.
doi:10.1016/j.ica.2009.02.046

complexes is often limited by their instability under physiological conditions, attributed to their high reduction potential and fast hydrolysis rate [17,21]. These problems can possibly be circumvented by forming gold(III) compounds with one or more multidentate nitrogen-donor ligands to enhance the stability of gold(III) complexes [21–23].

Recent reports that pyrazoles and substituted pyrazoles platinum complexes show cytotoxicity, while exhibiting lower toxicity than cisplatin [24,25], suggest that pyrazolyl ligands could stabilize gold(III) centers and overcome complex instability under physiological conditions. We have used pyrazolyl–pyridine ligands to prepare new platinum(II) and gold(III) complexes, as well as investigate their anticancer activity.

2. Results and discussion

2.1. Preparation of ligands

Six (pyrazolylmethyl)pyridine ligands were used to prepare platinum(II) and gold(III) complexes. These ligands were synthesized using the literature procedure reported for **L1** [26] (Scheme 1). These ligands had to be washed with copious amounts of water in order to remove the phase transfer catalyst used in their preparation which would otherwise coordinate to the metal precursors used in complexation of **L1–L6**. The two ligands prepared from 3,5-dimethypyrazole (**L1** and **L5**) were obtained as yellow and red oils, while those prepared from diphenylpyrazole (**L2** and **L6**), di-*tert*-butylpyrazole (**L3**) and *p*-tolylpyrazole (**L4**) were obtained as off-white to light brown solids. Ligands with bulky substituents on the pyrazolyl moiety (**L2**, **L3** and **L6**) required reaction times of at least 72 h to ensure reasonable yields and all of them were characterized by ^{1}H and ^{13}C NMR spectroscopy, and elemental analyses. The structure of **L6** was confirmed by X-ray crystallography (Fig. 1 and Table 1) and had no special features.

2.2. Preparation of (pyrazol-1-ylmethyl)pyridine platinum(II) complexes in water–acetone mixture: formation of acetonyl platinum(II) compounds

Ligands **L1**–**L3** reacted with $K_2[PtCl_4]$ in a mixture of water and acetone at 60 °C (Scheme 2). Except in the case of **L1** that afforded **1** as the sole product in quantitative yield, **L2** and **L3** produced mixtures of the dichloroplatinum(II) complexes **2** and **3**, and the monoacetonylplatinum(II) complexes **2a** and **3a**. The mixtures of the two types of complexes could be separated by recrystallization and revealed that the dichloro complexes were the major constituents of the mixtures. In one such separation acetonitrile solvated crystals of **2** could be isolated from the mixture as established from its crystal structure (Supplementary material CCDC 697856). Interestingly, all attempts to prepare what would have been **1a** resulted in isolation of the dichloroplatinum(II) complex **2**, most likely because it precipitated before it could be converted to its ketonyl analogue. Based on this observation it is reasonable to suggest that the formation of the monoacetonyl complexes is preceded by the formation of dichloro analogues. On prolonged heating (*ca.* 2 days) yields of **2** and **3** improved but with the formation of a more insoluble diacetonylplatinum(II) complex **2b** in the case of **2**. Acetonylplatinum(II) complexes have been shown to undergo disproportionation to form the diacetonylplatinum(II) complexes [27]. It can therefore be inferred that the diacetonylplatinum complex **2b** is formed as a secondary disproportionation product as depicted in Scheme 3.

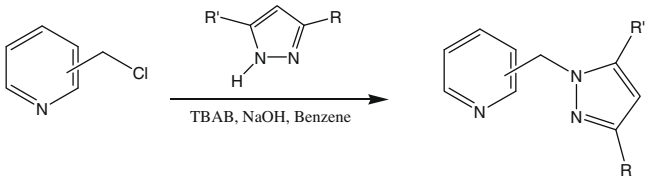

Position	R	R'	Ligand
2-	Me	Me	**L1**
2-	Ph	Ph	**L2**
2-	*t*Bu	*t*Bu	**L3**
2-	*p*-Tol	H	**L4**
4-	Me	Me	**L5**
4-	Ph	Ph	**L6**

Scheme 1. Preparation of ligands **L1**–**L6**.

^{1}H NMR spectrum of **3a** showed AB doublets for CH_2 protons in the ligand backbone at 6.57 and 5.72 ppm as two diastereotopic protons (axial and equatorial) that do not interconvert on the NMR time-scale. A distinguishing feature of spectrum of **3a** is a doublet resonance at 3.03 ppm, flanked by ^{195}Pt satellites, assigned to the methylene protons of the Pt–CH_2 bond. This chemical shift is comparable to a bipyridyl Pt–acetonyl complex reported by Falvello et al. [28]. Because of the poor solubility of **2a** evidence for the presence of the acetonyl functionality was provided by IR spectroscopy. A peak in the IR spectrum of **2a** at 1602 cm^{-1} was assigned to the ν(C=O) stretching mode of the acetonyl ligand. Peaks for related nitrogen-donor platinum–acetonyl complexes are $[Pt(CH_2COCH_3)Cl(bipy)]$ (1639 cm^{-1}) [29], *trans*-$[Pt(CH_2COCH_3)_2(bipy)]$ (1648 cm^{-1}) [30] and $[Pt(CH_2COCH_2CH_3)_2(bipy)]$ (1642 cm^{-1}) [30].

The molecular structure of **3a** (Fig. 2) confirmed presence of the acetonyl ligand. The platinum atom is coordinated to the (pyrazol-1-ylmethyl)pyridine ligand through the pyridyl nitrogen atom N(1), the pyrazolyl nitrogen N(3), to a chlorine atom, Cl(1), and to the acetonyl ligand through the methylene carbon C(18). The Pt–N bond distances of Pt(1)–N(1) (2.149 (3) Å) and Pt(1)–N(3) (2.021(3) Å) are typical, with the longer Pt–N distance being *trans* to the acetonyl ligand. This is longer than the bond distance observed for ketonyl bipyridine platinum complexes, with Pt–N bond distances of 2.082(3) and 2.091(3) Å for a diketonyl complex [31] and 2.082(11) Å for a monoketonyl complex [28]. The Pt(1)–C(18) distance of 2.077 (3) Å and the Pt(1)–Cl(1) distance of 2.3059 (8) Å are typical of these kinds of bonds. The C=O distance in the acetonyl ligand of 1.222 (4) Å is also typical of similar compounds [32–34].

2.3. Preparation of (pyrazol-1-ylmethyl)pyridine platinum(II) complexes in water–ethanol mixture

In view of the C–H activation observed with acetone, acetone was replaced with ethanol in order to isolate complexes **1**–**4** (Scheme 4). The complexes precipitated from the reaction medium and could easily be isolated by filtration. Complexes **1** and **4** were sparingly soluble but both **2** and **3** were soluble in common organic solvents, and could be characterized by ^{1}H and ^{13}C NMR spectroscopy, and in the case of **2** and **3** by X-ray crystallography. The ^{1}H NMR spectra of all complexes showed AB doublets for CH_2 protons in the ligand backbone with coupling constants of between 14.7 and 15.6 Hz, typical for *geminal* coupling. These peaks confirm the presence of two diastereotopic protons and are a distinguishing feature between the complexes and their respective ligands.

Molecular structures for **2** and **3** are shown in Figs. 3 and 4, respectively, and their crystallographic data is in Table 1. The

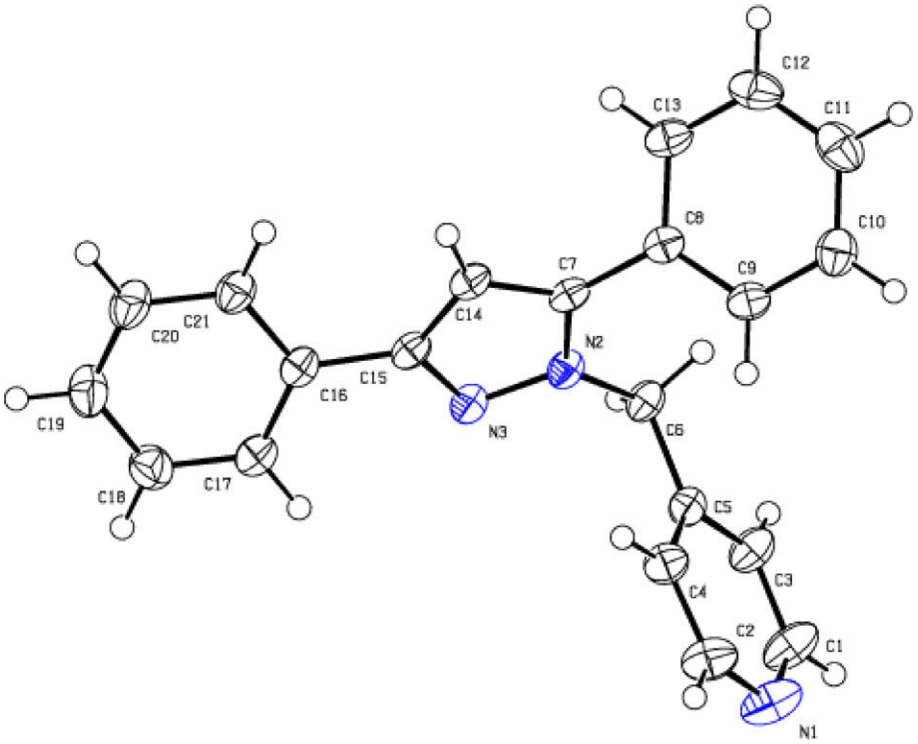

Fig. 1. Ortep diagram of **L6** drawn with 50% probability ellipsoids. Selected interatomic distances (Å) and angles (°) for **L6**. C(5)–C(6) 1.5135(17); C(14)–C(15) 1.4060(17); N(2)–N(3) 1.3630(14); C(1)–N(1) 1.343(2); C(2)–N(1) 1.3373(19); C(7)–N(2) 1.3643(15); C(15)–N(3) 1.3418(15); C(6)–N(2) 1.4598(15); N(2)–C(6)–C(5) 114.94(10), C(2)–N(1)–C(1) 115.70(12); N(3)–N(2)–C(7) 112.20(10); C(15)–N(3)–N(2) 104.84(10).

Table 1
Crystallographic data for **L6**, **2**, **3a**, **3**, **8** and **10**.

	L6	**2**	**3a**	**3**	**8**	**10**
Empirical formula	$C_{21}H_{17}N_3$	$C_{21}H_{17}Cl_2N_3Pt$	$C_{20}H_{30}ClN_3OPt$	$C_{17}H_{25}Cl_2N_3Pt$	$C_{16}H_{15}Au_2Cl_6N_3$	$C_{21}H_{17}Au\ Cl_3N_3$
Formula weight	311.38	577.37	559.01	537.39	855.94	614.69
T (K)	173(2)	105(2)	105(2)	105(2)	100(2)	100(2)
Wavelength (Å)	0.71073	0.71073	0.71073	0.71073	0.71073	0.71073
Crystal system	monoclinic	monoclinic	monoclinic	monoclinic	monoclinic	monoclinic
Space group	$P2_1/n$	$P2_1/n$	$P2_1/c$	$P2_1/n$	$P2_1/c$	$P2_1/n$
a (Å)	12.1849(7)	12.1148(8)	10.2878(7)	12.2277(9)	6.9788(4)	10.0555(5)
b (Å)	10.4719(6)	14.6424(9)	22.1057(15)	11.2407(8)	36.4603(18)	9.1926(4)
c (Å)	13.7416(8)	12.2761(8)	10.4044(7)	13.4521(10)	8.5149(4)	22.4962(11)
α (°)	90	90	90°	90	90	90
β (°)	110.875(3)	116.8030(10)	117.4910(10)	91.5010(10)	101.7540(10)	91.7560(10)
γ (°)	90	90	90	90	90	90
V (Å^3)	1638.32(16)	1943.7(2)	2099.0(2)	1848.3(2)	2121.18(19)	2078.49(17)
Z	4	4	4	4	4	4
Density (calculated) (Mg/m^3)	1.262	1.973	1.769	1.931	2.680	1.964
Absorption coefficient (mm^{-1})	7.600	7.505	6.826	7.883	14.581	7.476
Crystal size (mm^3)	0.50 × 0.46 × 0.30	0.46 × 0.15 × 0.14	0.27 × 0.11 × 0.06	0.21 × 0.12 × 0.08	0.43 × 0.32 × 0.25	0.39 × 0.35 × 0.29
Reflections collected	15 648	26 591	28 775	27 248	27 325	29 247
Absorption correction	multi-scan with SADABS	multi-scan with SADABS	empirical with SADABS	empirical with SADABS	multi-scan with SADABS	multi-scan with SADABS
Maximum and minimum transmission	0.978 and 0.940	0.4197 and 0.1297	0.6849 and 0.2601	0.5712 and 0.2883	0.1215 and 0.0619	0.2204 and 0.1586
Goodness-of-fit (GOF) on F^2	1.168	0.960	1.023	1.067	1.111	1.007
Final R indices [$I > 2\sigma(I)$]	R_1 = 0.0449, wR_2 = 0.1118	R_1 = 0.0153, wR_2 = 0.0394	R_1 = 0.0243, wR_2 = 0.0490	R_1 = 0.0307, wR_2 = 0.0636	R_1 = 0.0253, wR_2 = 0.0616	R_1 = 0.0181, wR_2 = 0.0440
R indices (all data)	R_1 = 0.0619, wR_2 = 0.1190	R_1 = 0.0173, wR_2 = 0.0405	R_1 = 0.0400, wR_2 = 0.0537	R_1 = 0.0575, wR_2 = 0.0752	R_1 = 0.0291, wR_2 = 0.0629	R_1 = 0.0189, wR_2 = 0.0443

geometry around both metals is distorted square-planar. While the metric parameters of **2** and **3** fall in the usual ranges, it is interesting to comment on the difference in the Pt(1)–N(3) bond lengths in the two complexes. The Pt(1)–N(3) bond in **2** is 0.022 Å shorter, and the difference is statistically significant. This fact is in accord with the ligand steric requirement expressed by their solid angles but in contrast to their minimum volumes [the volumes calculated assuming all space about the ligand is accessible by a probe atom or a solvent molecule]. Ligand **L2** shields 42.7% (5.36 sr) of the Pt1 coordination sphere while **L3** shields 44.5% (5.59 sr) [35]. The

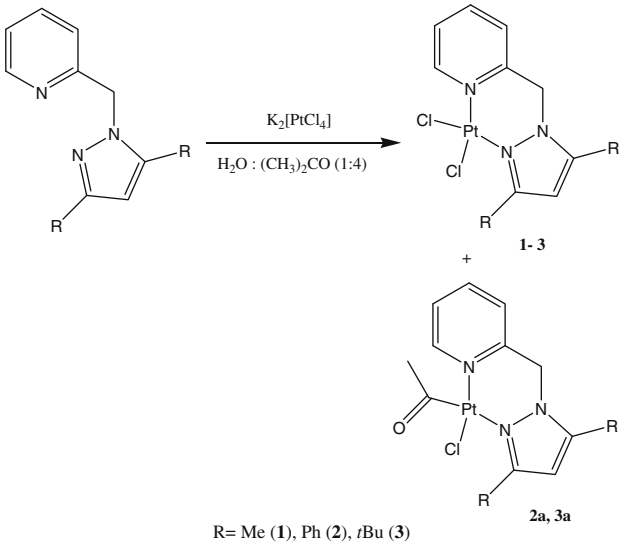

R= Me (**1**), Ph (**2**), *t*Bu (**3**)

Scheme 2.

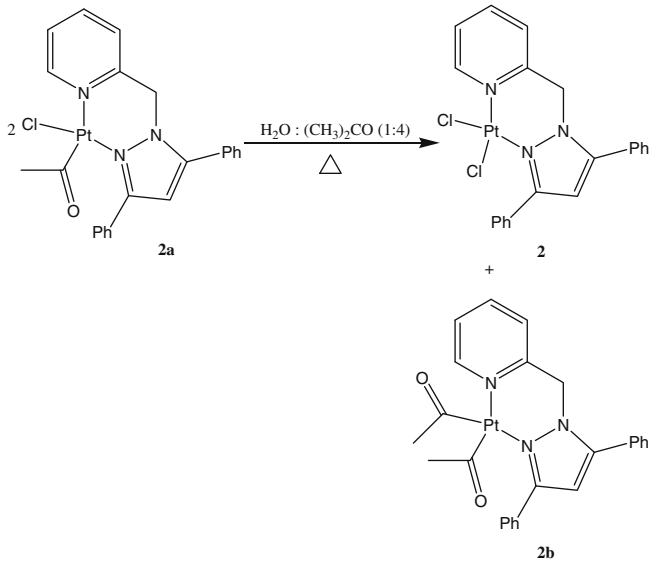

Scheme 3. Disproportionation of **2a** to a diacetonyl complex

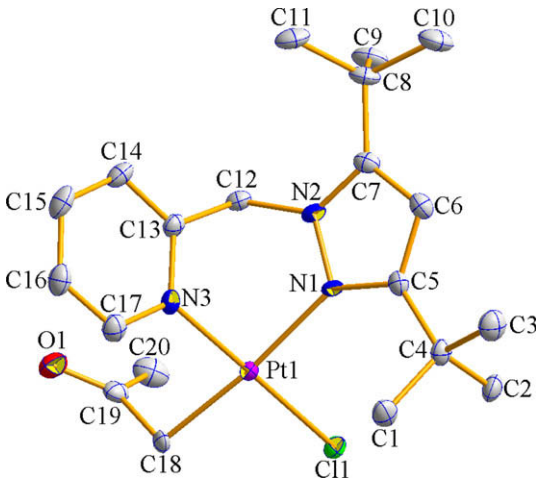

Fig. 2. A molecular drawing of **3a** drawn with 50% probability ellipsoids. All hydrogen atoms were omitted for clarity. Selected interatomic distances (Å) and angles (°) for **3a**: Pt(1)–N(1) 2.149(3); Pt(1)–N(3) 2.021(3); Pt(1)–C(18) 2.077(3); Pt(1)–Cl(1) 2.3059(8); O(1)–C(19) 1.222(4); N(3)–Pt(1)–C(18) 90.41(11); N(3)–Pt(1)–N(1) 85.17(10); C(18)–Pt(1)–Cl(1) 87.65(9); N(1)–Pt(1)–Cl(1) 96.50(7), C(18)–Pt(1)–N(1) 174.17(10); N(3)–Pt(1)–Cl(1) 175.73(7).

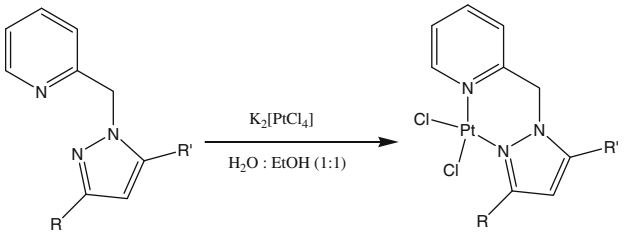

R	R'	Complex
Me	Me	**1**
Ph	Ph	**2**
*t*Bu	*t*Bu	**3**
p-tol	H	**4**

Scheme 4.

volume of **L2** (281.34(8) Å^3) exceeds that of **L3** (267.90(9) Å^3) by 13.44 Å^3, however, the bulkiness of the **L2** is due to the larger number of atoms in the Ph rings that do not play a role in shielding of the central metal. We also computed the "buried volumes" [36] of a 3.0 Å sphere about the central metals in **2** and **3** that can be used as a measure of steric crowding in coordination compounds. The "buried volume" for ligand **L2** is smaller (62.43(3) Å^3) than that for **L3** (63.78(3) Å^3), a result consistent with our ligand solid angle considerations [37].

It is instructive to compare and contrast the ligand solid angles in **3** and **3a** since both complexes contain ligand **L3**. The extent to which the bidentate **L3** shields the metal center in **3a** is 42.7% (5.34 sr), the ligand volume is 267.63(8) Å^3, and the "buried volume" of a 3.0 Å sphere about Pt1 in **3a** is 68.06(4) Å^3. The **L3** volumes computed for **3** and **3a** are in excellent agreement indicating that small conformational changes do not affect the ligand volume. The **L3**'s solid angle in **3a** is smaller than in **3** by 0.25 sr (or 1.8% less effective metal shielding) due to the longer Pt1–N(py) bond distance in **3a** positioned *trans* to the acetonyl ligand. It is well-known that metal–ligand distances may noticeably affect the solid angles. The presence of an acetonyl ligand in **3a** resulted in a substantially more congested environment (see the buried volumes) about the Pt center, however, the congestion does not manifest itself in an elongation of Pt–N(pz) and Pt–Cl bond distances. Thus, the larger Pt–N(py) distance in **3a** as compared to that in **3** is a consequence of the acetonyl *trans*-influence only, and not a result of unfavorable steric interactions among the ligands.

2.4. Preparation of gold(III) complexes

Addition of one equivalent of ethanolic solution of $H[AuCl_4] \cdot 4H_2O$ to solutions of the (pyrazol-1-ylmethyl)pyridine ligands produced new gold complexes **5–10** (Schemes 5 and 6). Interestingly, only the methylenic protons in **5** showed AB doublets in its ^{1}H NMR spectrum, reminiscent of the platinum complexes. It also took several microanalyses of samples **5–8** from different experiments to establish that there were two types of anions in the gold salts. Complexes **5** and **8** were found to have $[AuCl_4]^-$ as counter ions, whereas **6** and **7** had Cl^- as counter ions. This is not the first

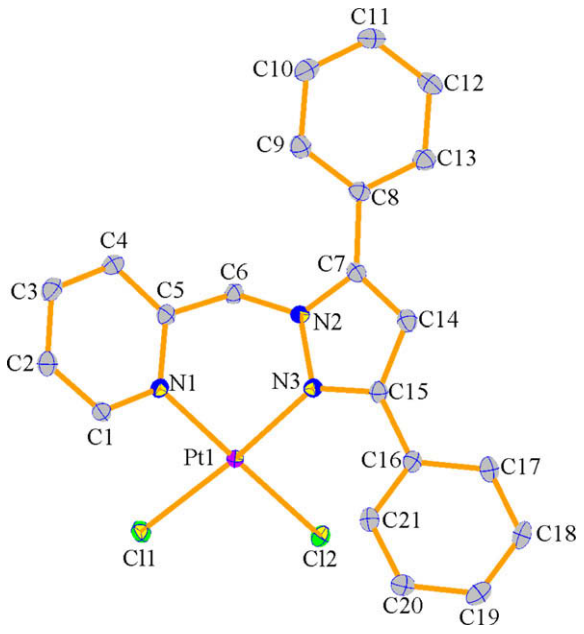

Fig. 3. A molecular drawing of **2** drawn with 50% probability ellipsoids. All hydrogen atoms were omitted for clarity. Selected interatomic distances (Å) and angles (°) for **2**: Pt(1)–N(1) 2.0220(17); Pt(1)–N(3) 2.0193(16); Pt(1)–Cl(1) 2.2902(5); Pt(1)–Cl(2) 2.2970(5); N(1)–Pt(1)–N(3) 87.02(7), N(1)–Pt(1)–Cl(2) 177.15(5); N(1)–Pt(1)–Cl(1) 89.19(5); N(3)–Pt(1)–Cl(2) 93.20(5); N(3)–Pt(1)–Cl(1) 175.72(5), Cl(1)–Pt(1)–Cl(2) 90.501(18).

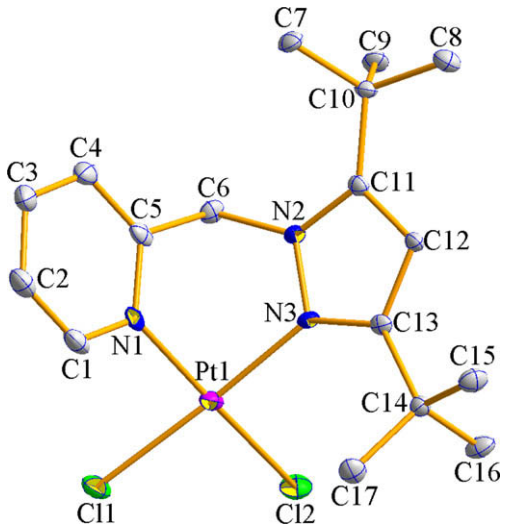

Fig. 4. A molecular drawing of **3** drawn with 50% probability ellipsoids. Selected interatomic distances (Å) and angles (°) for **3**: Pt(1)–N(1) 2.012(4); Pt(1)–N(3) 2.041(4); Pt(1)–Cl(1) 2.2895(11), Pt(1)–Cl(2) 2.3069(12), N(1)–Pt(1)–N(3) 85.53(14), N(1)–Pt(1)–Cl(2) 173.99(11), N(3)–Pt(1)–Cl(1) 175.38(10); N(1)–Pt(1)–Cl(1) 90.18(10), N(3)–Pt(1)–Cl(2) 94.74(10), Cl(1)–Pt(1)–Cl(2) 89.70(4).

example where different counter ions are formed in a gold complex involving bidentate nitrogen ligands. Shi et al. [38] have made similar observations for 1,4,7-triazacyclonane gold(III) salts, but for these gold salts the stoichiometry of the reaction influenced the cation formed. In reactions where ligand to $H[AuCl_4]$ was 1:1 the counter ion is Cl^- and for 2:1 ratio the counter ion was $[AuCl_4]^-$. However, using the exact stoichiometry in our reactions did not show a detectable impact on the nature of the counter ions observed for **5–8**. It is not clear to us what dictates the nature of the counter ion formed.

It is plausible that the formation of the gold salts **5**–**8** are preceded by the formation of a neutral trichlorogold(III) intermediate,

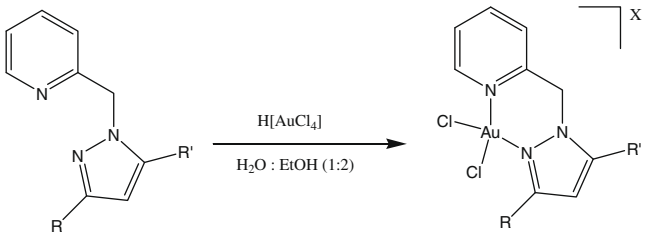

R	R'	X	Complex
Me	Me	$[AuCl_4]^-$	**5**
Ph	Ph	Cl^-	**6**
*t*Bu	*t*Bu	Cl^-	**7**
p-Tol	H	$[AuCl_4]^-$	**8**

Scheme 5.

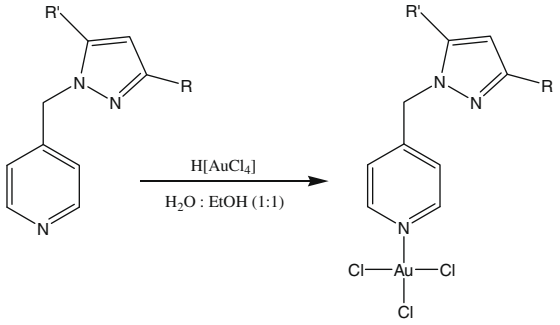

R	R'	Complex
Me	Me	**9**
Ph	Ph	**10**

Scheme 6.

which is then converted into the isolated cationic species; stabilized by the pyrazolyl unit (Scheme 7). By modifying the connectivity within the bidentate ligand and preventing its binding to the gold centre in a k^2-fashion we could isolate trichlorogold(III) complexes with ligands **L5** and **L6**. The X-ray structure of **10** confirmed the formation of the expected trichlorogold(III) complex and supports the proposed pathway to the formation of the gold(III) salts **5–8** (Scheme 7).

The X-ray structure of **8** confirmed that the cationic salt **8** has $[AuCl_4]^-$ as a counter-ion. The six-membered metallacycle is in a boat conformation, whereas the coordination geometry about the gold is a distorted square-planar. The two heterocyclic rings are not coplanar with the coordination plane of the gold centre. The Au(1)–N(1) bond distance is (2.036(4) Å) is found to be longer than the Au(1)–N(3) bond [2.018(4) Å]. As expected, the Au(1)–Cl(1) bond [2.2686(12) Å] which is *trans* to the pyrazolyl nitrogen N(3), is slightly longer than the Au(1)–Cl(2) bond of 2.2598(12) Å, *trans* to the pyridine nitrogen N(1). This can be attributed to a greater *trans* influence of the pyrazolyl nitrogen. The Au–N and Au–Cl distances are similar to Au–N [2.028(6)°] and Au–Cl [2.251(2)°] those found for $[AuCl_2(N^N)][AuCl_4]$ where N^N = *N*-isopropyl-*N*-2-ethylpyridine [39], and other related gold(III) compounds [22].

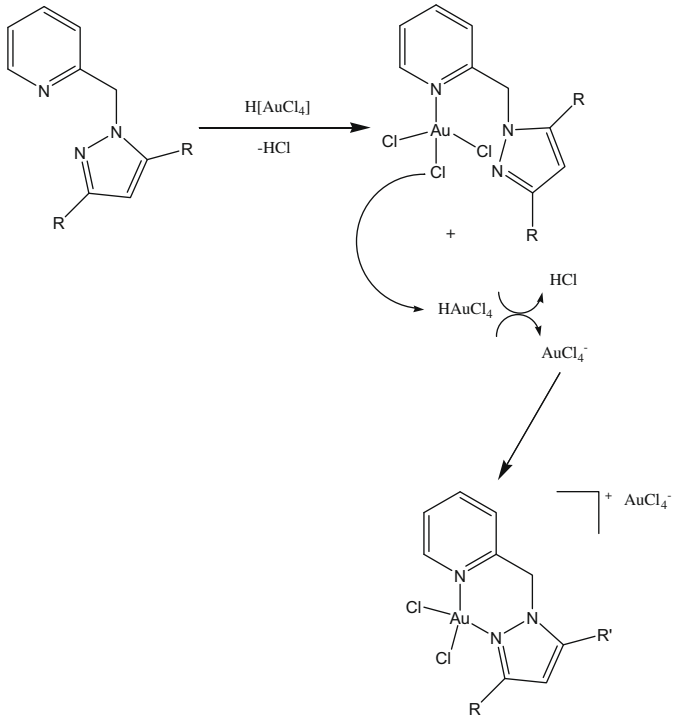

Scheme 7.

Complex **10** is also square-planar, with the gold atom coordinated to three chlorine atoms and the nitrogen of the pyridine ligand. It is well-known that the pyrazolyl ring nitrogens are more weakly coordinating to metal centres and also less basic than the pyridyl ring nitrogen [40], and it is thus no surprise that the gold(III) atom is bound through the nitrogen of the pyridine. The Au–N(1) distance of 2.029(2) Å is similar to those found in gold(III) complexes containing a pyridine ligand which is not strained [41–43]. The distance between Au–Cl(2) distance *trans* to the pyridine nitrogen of 2.261(2) Å is slightly shorter than those of Au(1)–Cl(1) (2.2811(8) Å and Au(1)–Cl(3) (2.2813(8) Å) bonds which are opposite to one another, owing to the reciprocal *trans* influence of Cl atoms [44]. The Au–N and Au–Cl bond lengths are in the expected regions for gold(III) complexes [41–43] (see Figs. 5 and 6).

2.5. Cytotoxicity studies

The cytotoxicity of ligands **L2** and **L4** and complexes **1–10** were evaluated against HeLa (Human adenocarcinoma of the cervix) cancer cell line using cisplatin as standard. For comparison purposes, the cytotoxic activity of cisplatin was also evaluated under the same experimental conditions. The results from these experiments are summarized as bar charts (Figs. 7 and 8). The inhibition of the growth of normal cells by the complexes tested was also measured by employing human lymphocytes (PBMC) cells, using the same procedure for the HeLa cells, except that treated PBMC cells were incubated for 3 days and not 7 days for the HeLa cells. This allowed for the determination of tumor specificity, which was calculated using Eq. (1)

$$TS = \frac{\text{Mean } IC_{50} \text{ of the normal cells(stimulated + resting lymphocytes)}}{\text{Mean } IC_{50} \text{ of the cancer cells}} \quad (1)$$

In doing so, the lymphocytes were divided into two. The first was normal cells that were stimulated using PHA-P so as to increase their proliferation rate (stimulated lymphocytes) and the second was un-stimulated normal cells (resting lymphocytes).

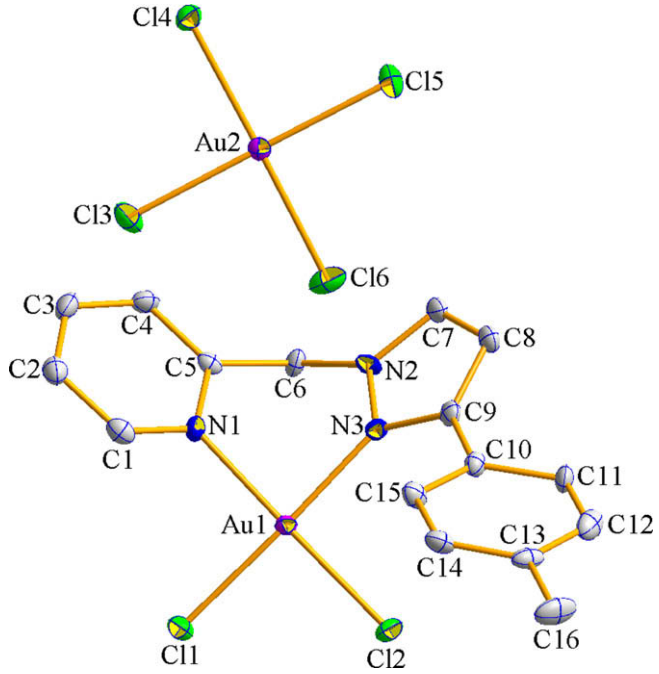

Fig. 5. An ORTEP diagram of **8** drawn with 50% probability ellipsoids. Selected interatomic distances (Å) and angles (°) for **8**. Au(1)–N(1) 2.036(4); Au(1)–N(3) 2.018(4); Au(1)–Cl(1) 2.2686(12); Au(1)–Cl(2) 2.2598(12); N(3)–Au(1)–Cl(1) 175.82(12); N(1)–Au(1)–Cl(2) 178.12(13); N(3)–Au(1)–N(1) 86.73(17).

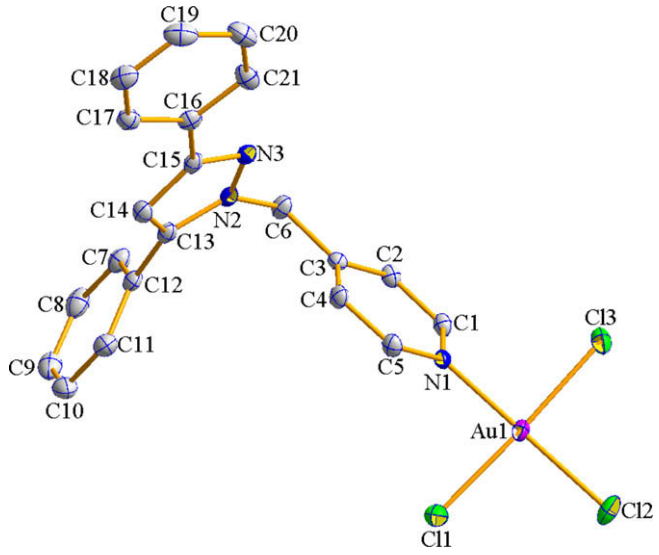

Fig. 6. An ORTEP diagram of **10** drawn with 50% probability ellipsoids. Selected interatomic distances (Å) and angles (°) for **10**. Au(1)–N(1) 2.029(2); Au(1)–Cl(1) 2.2811(8); Au(1)–Cl(2) 2.2681(8); Au(1)–Cl(3) 2.2813(8); N(1)–Au(1)–Cl(2) 178.60(7); Cl(1)–Au(1)–Cl(3) 176.79(3), Cl(2)–Au(1)–Cl(1) 91.24(3); Cl(2)–Au(1)–Cl(3) 91.26(3); N(1)–Au(1)–Cl(3) 88.43(7); N(1)–Au(1)–Cl(1) 89.11(7).

For the platinum complexes (Fig. 7), complexes bearing alkyl substituents on the pyrazolyl ring (**1** and **3**) were less active than those with aryl substituents (**2** and **4**). Although in terms of IC_{50} values, activity of **2** (IC_{50} = 3.849 μM) and **4** (IC_{50} = 8.920 μM) were approximately eight and nineteen times lower than that of cisplatin, they were much better than those exhibited by all other compounds tested (Figs. 7 and 8). Despite their better cytotoxicity both were found to show poor selectivity, killing both normal and deceased cells indiscriminately. On the other hand, the gold(III)

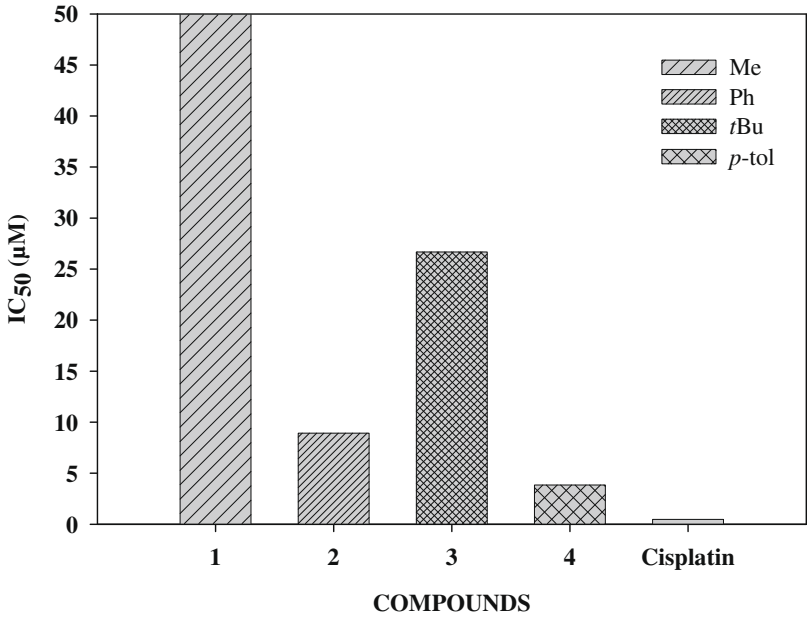

Fig. 7. Cytotoxicity of (pyrazolylmethyl)pyridine platinum(II) complexes

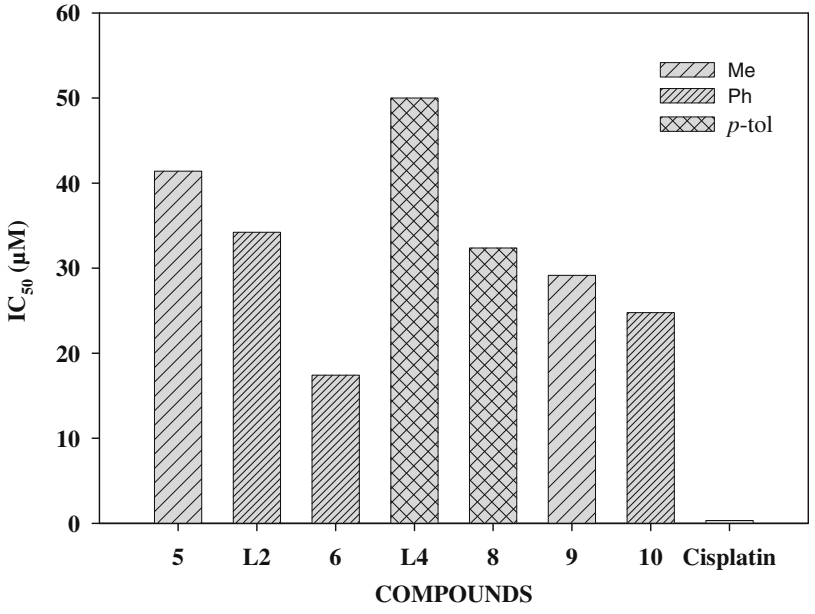

Fig. 8. Cytotoxicities of (pyrazolylmethyl)pyridine ligands and their gold(III) complexes.

complexes **5–10** (the best IC_{50} of 18.050 μM was for **6**) exhibited much lower cytotoxicity compared to cisplatin, but their cytotoxicities were better than the free ligands. The very low cytotoxcity of the gold complexes could be due to the low stability of gold(III) which generally reduce to gold(I). We have recently shown that the reduction of the gold(III) complex, $[AuCl_2(3,5\text{-}Me_2bpza)]Cl$ (bpza = bis(pyrazolyl) acetic acid), is very fast ($k_1 = 0.8\ M^{-1}\ s^{-1}$ at 293 K; followed by a much slower reaction of the ensuing gold(I) complex with L-cysteine ($k_2 = 300.8\ M^{-1}\ s^{-1}$) [45]. A similar reduction process is when the gold(III) complexes **5–10** were tested, since in the biological milleu used in the testing such reduction is possible and could explain the low activity of complexes **5–10**.

3. Conclusions

In preparing the platinum(II) complexes the choice of solvent is crucial in determining the products formed. When a mixture of water–acetone is used acetonylplatinum(II) complexes are formed, whereas the use of water–ethanol mixture affords the desired platinum(II) complexes, **1–4**. The C–H bonds α to an oxygen atom in acetone were activated in forming the acetonylplatinum(II)

complexes whereas unactivated C–H bonds in ethanol were neither attacked nor oxidized.

Two types of novel gold complexes were also prepared. The bidentate cationic gold(III) complexes (**5–8**) bind through both the pyridine and pyrazole nitrogen atoms, while the neutral monodentate gold(III) complexes, **9** and **10**, bind exclusively through the pyridine nitrogen atom. The gold complexes showed low cytotoxicity when tested against HeLa cells. Some of the platinum complexes showed good anticancer activity, but unfortunately exhibited low tumor specificity.

4. Experimental

4.1. Materials and instrumentation

All manipulations were performed under a dry, deoxygenated nitrogen atmosphere using standard Schlenk techniques. NMR spectra were recorded on a Gemini 2000 instrument. The chemical shifts are reported in δ (ppm) referenced to residual ^{1}H and ^{13}C signals of deuterated chloroform as internal standard. Hexane, benzene, toluene, and diethyl ether were purified by distillation from sodium benzophenone ketyl under a nitrogen atmosphere. All other solvents were of reagent grade and were used without further purification, unless oxygen-free solvent was needed, then the solvent was purged with nitrogen for ca. 15 min. Picolylchloride hydrochloride and 4-(bromomethyl)pyridine hydrobromide and cisplatin were obtained from Aldrich, while *p*-tolylpyrazole was purchased from Acros. Phosphate Buffered Saline (PBS), Eagle's RPMI-1640 medium, 3-(4,5-dimethylthiazol-2-yl)-2,5-diphenyltetrazolium bromide (MTT) kit, phytohemagglutinin-protein form (PHA-P) and the 96-well flat-bottomed culture plates were all purchased from BD Biosciences Ltd. All chemicals were used as received. Diphenylpyrazole [46] and di-*tert*-butylpyrazole [47] were prepared following literature procedures.

4.2. Preparation of ligands

4.2.1. Synthesis of 2-(3,5-diphenylpyrazol-1-ylmethyl)pyridine (*L2*)

A mixture of 2-picolylchloride hydrochloride (0.25 g, 1.53 mmol) and 3,5-diphenylpyrazole (0.34 g, 1.53 mmol) was dissolved in benzene (40 mL), to which 40% aqueous NaOH (12 mL) and 10 drops of 40% aqueous tetrabutylammonium bromide (TBAB) was added. The mixture was refluxed for 72 h after which the organic phase was extracted and evaporated under reduced pressure to afford yellow oil. The oil was redissolved in dichloromethane and washed with water to remove the phase transfer catalyst and the organic extract evaporated to give an off-white solid. Yield = 0.41 g, 84%. ^{1}H NMR (300 MHz, $CDCl_3$, 25): δ 8.57 (d, $^3J_{H,H}$ = 4.40 Hz, 1H, H_6-py), 7.90 (d, $^3J_{H,H}$ = 1.40 Hz, 1H, H_3-py), 7.86 (s, 1H, H_5-py), 7.58 (td, $^3J_{H,H}$ = 7.60 Hz, 1H, H_4-py), 7.39 (m, 10H, Ph), 6.70 (s, 1H, H_4-pz), 5.54 (s, 2H, $-CH_2-$). $^{13}C\{^1H\}$ NMR (75 MHz, $CDCl_3$, 25): δ 157.7 (C_2-py), 151.4 (C_3-pz), 149.3 (C_6-py), 145.9 (C_5-pz), 137.0 (Ph), 133.2 (C_4-py), 130.2 (Ph), 128.7 (Ph), 128.6 (Ph), 127.8 (Ph), 125.7 (C_3-py), 122.3 (C_5-py), 103,7 (C_4-pz), 55.0 ($-CH_2$) ppm. *Anal.* Calc. for $C_{21}H_{17}N_3$: C, 81.00; H, 5.50; N, 13.49. Found: C, 81.10; H, 5.37; N, 13.05%.

Ligands **L3**–**L6** were prepared following the same procedure for **L2**.

4.2.2. Synthesis of 2-(3,5-di-tert-butylpyrazol-1-ylmethyl)-pyridine (*L3*)

Compound **L3** was prepared from picolyl chloride hydrochloride (0.50 g, 3.05 mmol) and 3,5-*tert*-butylpyrazole (0.55 g, 3.05 mmol), and the mixture was refluxed for 72 h. The product was obtained as a white solid. Yield = 0.63 g, 76%. ^{1}H NMR ($CDCl_3$): δ 8.52 (d, $^3J_{H,H}$ = 6.90 Hz, 1H, py), 7.57 (q, $^3J_{H,H}$ = 5.40 Hz, 1H, py), 7.13, (t, $^3J_{H,H}$ = 5.40 Hz, 1H, py) 6.48 (d, $^3J_{H,H}$ = 8.10 Hz, 1H, py), 5.89 (s, 1H, pz), 5.57 (s, 2H, CH_2-), 1.32 (s, 9H, *t*Bu), 1.25 (s, 9H, *t*Bu). *Anal.* Calc. for $C_{17}H_{25}N_3$: C, 75.23; H, 9.28; N, 15.48. Found: C, 75.18; H, 9.66; N, 15.52%.

4.2.3. Synthesis of 2-(3-para-tolylpyrazol-1-ylmethyl)pyridine (*L4*)

Compound **L4** was prepared from picolyl chloride hydrochloride (0.30 g, 2.33 mmol) and 3-tolylpyrazole (0.370 g, 2.33 mmol). The product was obtained as a light brown solid. Yield = 0.373 g, 63%. ^{1}H NMR ($CDCl_3$): δ 8.58 (d, $^3J_{H,H}$ = 4.5 Hz, 2H, py), 7.73 (s, 1H, py), 7.70 (s, 1H, py), 7.64 (t, $^3J_{H,H}$ = 4.50 Hz, 1H, py), 7.53 (d, $^3J_{H,H}$ = 2.10 Hz, 1H, pz), 7.21 (d, $^3J_{H,H}$ = 7.80 Hz, 3H, *p*-tolpz), 7.04 (d, $^3J_{H,H}$ = 7.8 Hz, 1H, *p*-tolpz), 6.59 (d, $^3J_{H,H}$ = 2.10 Hz, 1H, pz), 5.50 (s, 2H, CH_2-), 2.37 (s, 3H, Me-*p*-tolpz). $^{13}C\{^1H\}$ NMR (300 MHz, $CDCl_3$): δ 156.81 (C_2-py), 152.03 (C_3-pz), 149.19 (C_6-py), 137.33 (*p*tol-C_{para}), 137.08 (C_4-py), 131.26 (C_1-*p*tol), 130.53 (C_5-pz), 129.21 (*p*tol-C_{meta}), 125.48 (*p*tol-C_{ortho}), 122.63 (C_3-Py), 121.58 (C_5-py), 103.3 (C_4-pz), 57.56 ($-CH_2$), 21.22 (Me-*p*tol) ppm. *Anal.* Calc. for $C_{16}H_{15}N_3$: C, 77.08; H, 6.06; N, 16.85. Found: C, 76.38; H, 6.10; N, 16.83%.

4.2.4. Synthesis of 4-(3,5-dimethylpyrazol-1-ylmethyl)pyridine (*L5*)

Compound **L5** was prepared from 4-(bromomethyl)pyridine hydrobromide (1.00 g, 3.95 mmol) and 3,5-dimethylpyrazole (0.380 g, 3.95 mmol). The product was obtained as red oil. Yield = 0.70 g, 95%. ^{1}H NMR ($CDCl_3$): δ 8.53 (d, $^3J_{H,H}$ = 5.40 Hz, 2H, $H_{2,6}$-py), 6.93 (d, $^3J_{H,H}$ = 6.20 Hz, 2H, $H_{3,5}$-py), 5.89 (s, 1H, H_4-pz), 5.22 (s, 2H, $-CH_2-$), 2.24 (s, 3H, Me-pz), 2.14 (s, 3H, Me-pz). $^{13}C\{^1H\}$ NMR ($CDCl_3$): δ 148.5 (C_3-pz), 147.60 ($C_{2,6}$-py), 138.65 (C_4-py), 134.0 ($C_{3,5}$-py), 105.4 (C_4-pz), 49.5 ($-CH_2$), 13.0 (Me-pz), 10.0 (Me-pz) ppm.

4.2.5. Synthesis of 4-(3,5-diphenylpyrazol-1-ylmethyl)pyridine (*L6*)

Compound **L6** was prepared from 4-(bromomethyl)pyridine hydrobromide (0.98 g, 3.88 mmol) and 3,5-diphenylpyrazole (0.85 g, 3.88 mmol), the mixture was refluxed for 72 h. The product was obtained as colorless crystals. Yield = 0.78 g, 65%. ^{1}H NMR (300 MHz, $CDCl_3$, 25 °C): δ 8.55 (dd, $^3J_{H,H}$ = 2.80 Hz, $^4J_{H,H}$ = 1.60 Hz, 2H, $H_{3,5}$-py), 7.88 (d, 2H, Ph, $^3J_{H,H}$ = 10.0 Hz), 7.36 (m, 8H, Ph), 7.06 (d, 2H, $H_{2,6}$-py, $^3J_{H,H}$ = 5.80 Hz), 6.71 (s, 2H, H_4-pz), 5.41 (s, 2H, $-CH_2-$). $^{13}C\{^1H\}$ NMR (75 MHz, $CDCl_3$, 25 °C): δ 151.5 (C_3-pz), 150.1 ($C_{2,6}$-py), 146.6 (C_5-pz), 145.7 (C_4-py), 133.0 (Ph), 130.0 (Ph), 128.9 (Ph), 128.8 (Ph), 128.6 (Ph), 127.9 (Ph), 125.6 (Ph), 121.4 ($C_{3,5}$-py), 103.9 (C_4-pz), 52.1 ($-CH_2$) ppm. *Anal.* Calc. for $C_{21}H_{17}N_3$: C, 81.00; H, 5.50; N, 13.49. Found: C, 80.75; H, 5.42; N, 13.47%.

4.3. Preparation of (pyrazolylmethyl)pyridine platinum(II) complexes

4.3.1. Synthesis of dichloro[2-(3,5-dimethylpyrazol-1-ylmethyl)pyridine]platinum(II) (*1*)

To a stirred solution of **L1** (0.094 g, 0.50 mmol) in ethanol (5 mL) was added dropwise an aqueous solution (5 mL) of $K_2[PtCl_4]$ (0.21 g, 0.50 mmol). The resulting solution was heated at 60 °C for 16 h, after which the precipitated yellow solid was collected by filtration, washed with water and ether and dried. Yield = 0.19 g, 85%. ^{1}H NMR (300 MHz, DMSO-d_6, 25 °C): δ 8.94 (d, $^3J_{H,H}$ = 6.90 Hz, 1H, py), 8.13 (t, $^3J_{H,H}$ = 7.80 Hz, 1H, py), 7.94 (d, $^3J_{H,H}$ = 6.90 Hz, 1H, py), 7.56 (t, $^3J_{H,H}$ = 7.80 Hz, 1H, py), 6.13 (s, 1H, pz), 5.84 (d, $^2J_{H,H}$ = 15.6 Hz, 1H, $-CH_2$), 5.65 (d, $^2J_{H,H}$ = 15.6 Hz, 1H, $-CH_2$,), 2.43 (s, 3H, Me), 2.41 (s, 3H, Me). $^{13}C\{^1H\}$ NMR (75 MHz, DMSO-d_6, 25 °C): δ 153.5 (C_2-py), 152.5 (C_3-pz), 150.9 (C_6-py), 142.5 (C_4-py), 140.5, 126.2 (C_3-py), 125.7 (C_5-py), 107.7 (C_4-pz), 52.6 ($-CH_2$), 13.9 (Me), 11.2 (Me) ppm. *Anal.* Calc. for $C_{11}H_{13}Cl_2N_3Pt$: C, 29.15; H, 2.89; N, 9.27. Found: C, 28.90; H, 2.79; N, 9.02%.

*4.4. Compounds **2–4** were prepared following the same procedure for **1***

*4.4.1. Synthesis of dichloro 2-(3,5-diphenylpyrazol-1-ylmethyl)pyridine platinum(II) (**2**)*

Compound **2** was prepared using **L2** (0.10 g, 0.33 mmol) and $K_2[PtCl_4]$ (0.14 g, 0.33 mmol). The product was product was obtained as a cream white solid. Yield = 0.17 g, 86%. Crystals of **2** suitable for X-ray structure determinations were obtained from acetonitrile solution by slow evaporation of solvent at room temperature in the dark. ^{1}H NMR (300 MHz, CD_3CN, 25 °C): δ 9.20 (d, $^3J_{H,H}$ = 5.10 Hz, 1H, py), 8.28 (d, $^3J_{H,H}$ = 7.80 Hz, 1H, py), 8.27 (d, $^3J_{H,H}$ = 7.80 Hz,1H, py), 8.00 (t, $^3J_{H,H}$ = 7.50 Hz, 1H, py), 7.54 (m, 10H, Ph), 6.77 (s, 1H, pz), 6.20 (d, $^2J_{H,H}$ = 15.3 Hz, 1H, –CH_2), 5.34 (d, $^2J_{H,H}$ = 15.3 Hz, 1H, –CH_2). ^{13}C{^{1}H} NMR (75 MHz, CD_3CN, 25 °C): δ 154.8 (C_2-py), 141.3 (C_3-py), 131.3 (C_6-py), 130.4 (C_4-py), 130.2 (Ph), 129.8 (Ph), 128.9 (Ph), 127.3 (Ph), 126.7 (Ph), 108.9 (C_4-pz), 55.7 (–CH_2) ppm. *Anal.* Calc. for $C_{21}H_{17}Cl_2N_3Pt$: C, 43.69; H, 2.97; N, 7.28. Found: C, 42.06; H, 2.99; N, 6.68%.

*4.4.2. Synthesis of dichloro 2-(3,5-di-tert-butylpyrazol-1-ylmethyl)pyridineplatinum(II) (**3**)*

Compound **3** was prepared from **L3** (0.06 g, 0.22 mmol) and K_2PtCl_4 (0.09 g, 0.22 mol). The product was product was obtained as a light brown solid. Yield = 0.10 g, 86%. Recrystallization from a mixture of dichloromethane and hexane in the dark at room temperature gave colorless crystals of **3** suitable for X-ray structure determination. ^{1}H NMR (300 MHz, $CDCl_3$, 25 °C): δ 9.12 (d, $^3J_{H,H}$ = 6.00 Hz, 1H, py), 7.91 (t, $^3J_{H,H}$ = 6.30 Hz, 1H,py), 7.49 (d, $^3J_{H,H}$ = 7.50 Hz, 1H, py), 7.41 (t, $^3J_{H,H}$ = 6.30 Hz, 1H, py), 6.66 (d, $^2J_{H,H}$ = 14.7 Hz, 1H, –CH_2), 6.00 (s, 1H, pz), 5.52 (d, $^2J_{H,H}$ = 14.7 Hz, 1H, –CH_2), 1.69 (s, 9H, *t*Bu), 1.45 (s, 9H, *t*Bu). ^{13}C{^{1}H} NMR (75 MHz, $CDCl_3$, 25 °C): δ 154.2 (C_2-Py), 148.5 (C_3-pz), 139.2 (C_6-py), 126.1 (C_3-py), 124.1 (C_5-py), 104.7 (C_4-pz), 53.4 (–CH_2), 31.5 (*t*Bu), 30.1 (*t*Bu) ppm. *Anal.* Calc. for $C_{17}H_{25}Cl_2N_3Pt$: C, 38.00; H, 4.69; N, 7.82. Found: C, 37.49; H, 4.64; N, 7.65%.

*4.4.3. Synthesis of **3a***

To a refluxing stirred solution of **L3** (0.10 g, 0.37 mmol) in acetone (20 mL) was added dropwise with stirring, an aqueous solution (5 mL) of K_2PtCl_4 (0.15 g, 0.37 mmol). The resulting solution was heated at 60 °C for 16 h. The precipitated green fluffy solid was collected by filtration, washed with water and ether and dried. Yield = 0.11 g, 54%. Recrystallization from a mixture of dichloromethane and hexane in the dark at room temperature gave colorless crystals of **3a** suitable for X-ray structure determination. ^{1}H NMR (300 MHz, CD_3CN, 25 °C): δ 8.88 (d, $^3J_{H,H}$ = 6.30 Hz, 1H, py,), 7.99 (t, $^3J_{H,H}$ = 6.00 Hz, 1H, py), 7.67 (d, $^3J_{H,H}$ = 8.1 Hz, 1H, py), 7.45 (t, $^3J_{H,H}$ = 6.00 Hz, 1H, py), 6.57 (d, $^2J_{H,H}$ = 15.3 Hz, 1H, –CH_2), 6.19 (s, 1H, pz), 5.72 (d, $^2J_{H,H}$ = 15.3 Hz, 1H, –CH_2), 3.03 (s, 1H, –CH_2-Pt), 2.98 (s, 1H, –CH_2-Pt), 1.68 (s, 1H, Me), 1.55 (s, 9H, *t*Bu), 1.41 (s, 9H, *t*Bu). ^{13}C{^{1}H} NMR (75 MHz, CD_3CN, 25 °C): δ 180.5 (–C=O), 154.5 (C_2-py), 141.3 (C_3-py), 127.2 (C_6-py), 126.1 (C_4-py), 105.9 (C_4-pz), 56.8 (–CH_2), 53.9 (Pt-CH_2), 34.1 (*t*Bu), 32.7(*t*Bu), 31.8 (*t*Bu), 30.2 (*t*Bu), 20.6 (Me) ppm. *Anal.* Calc. for $C_{19}H_{28}ClN_3OPt$: C, 41.87; H, 5.18; N, 7.71. Found: C, 42.03; H, 5.37; N, 7.87%.

*4.4.4. Synthesis of dichloro 2-(3-p-tolylpyrazol-1-ylmethyl)pyridineplatinum(II) (**4**)*

Compound **4** was prepared from **L4** (0.09 g, 0.35 mmol) and $HAuCl_4$ (0.14 g, 0.35 mmol). The product was product was obtained as a pale brown solid. Yield = 0.14 g, 80%. *Anal.* Calc. for $C_{16}H_{15}N_3PtCl_2$: C, 37.29; H, 2.93; N, 8.15. Found: C, 37.45; N, 2.91; H, 7.81%.

4.5. Preparation of (pyrazolylmethyl)pyridine gold(III) complexes

*4.5.1. Synthesis of dichloro[2-(3,5-dimethylpyrazol-1-ylmethyl)pyridine]gold(III) tetrachloro-aurate (**5**)*

To a solution of **L1** (0.20 g, 1.07 mmol) in ethanol (10 mL) was added dropwise an aqueous solution (5 mL) of $H[AuCl_4] \cdot 4H_2O$ (0.44 g, 1.07 mmol). The solution became turbid followed by precipitation of the expected product within 5 min. After 30 min the yellow precipitate was filtered, washed with copious amounts of water and diethyl ether, and then dried under vacuum. Yield = 0.15 g, 35%. ^{1}H NMR (300 MHz, CD_3CN, 25 °C): δ 9.04 (d, $^3J_{H,H}$ = 6.0 Hz, 1H, py), 8.35 (t, $^3J_{H,H}$ = 7.8 Hz, 1H, py), 8.00 (d, $^3J_{H,H}$ = 7.8 Hz, 1H, py), 7.86 (t, 1H, py, $^3J_{H,H}$ = 7.5 Hz), 6.34 (s, 1H, pz), 5.82 (d, $^2J_{H,H}$ = 16.5 Hz, 1H, –CH_2) 5.65 (d, $^2J_{H,H}$ = 16.5 Hz, 1H, –CH_2), 2.59 (s, 3H, Me), 2.48 (s, 3H, Me). ^{13}C{^{1}H} NMR (75 MHz, CD_3CN, 25 °C): δ 153.2 (C_2-py), 152.3 (C_3-pz), 150.3 (C_6-py), 147.8 (C_5-pz), 146.5 (C_4-py), 129.7 (C_3-py), 129.4 (C_5-py), 110.7 (C_4-pz), 53.7 (–CH_2), 14.7 (Me), 12.2 (Me) ppm. *Anal.* Calc. for $C_{11}H_{13}Au_2Cl_6N_3$: C, 16.64; H, 1.65; N, 5.29. Found: C, 16.91; H, 1.58; N, 5.11%.

Complexes **6–8** were prepared following the same procedure used for **5**.

*4.5.2. Synthesis of dichloro[2-(3,5-diphenylpyrazol-1-ylmethyl)pyridine]gold(III) chloride (**6**)*

Compound **6** was prepared from **L2** (0.15 g, 0.48 mmol) and $H[AuCl_4] \cdot 4H_2O$ (0.20 g, 0.48 mmol). The product precipitated as a yellow solid but was obtained as orange solid after recrystallization from dichloromethane and hexane. Yield = 0.13 g, 44%. ^{1}H NMR (300 MHz, $CDCl_3$, 25 °C): δ 8.73 (d, $^3J_{H,H}$ = 5.10 Hz, 1H, py), 8.04 (t, $^3J_{H,H}$ = 7.8 Hz, 1H, py), 7.89 (d, $^3J_{H,H}$ = 5.10 Hz, 1H, py), 7.62 (t, $^3J_{H,H}$ = 7.80 Hz, 1H, py), 7.45 (m, 10H, Ph), 6.81 (s, 1H, pz), 6.06 (s, 2H, –CH_2). ^{13}C{^{1}H} NMR (300 MHz, $CDCl_3$, 25 °C): δ 157.7 (C_2-py), 151.4 (C_3-pz), 149.3 (C_6-py), 145.9 (C_5-pz), 137.0 (Ph), 133.2 (C_4-py), 130.2 (Ph), 128.7 (Ph), 128.6 (Ph), 127.8 (Ph), 125.7 (C_3-py), 122.3 (C_5-py), 103,7 (C_4-pz), 55.0 (–CH_2) ppm. *Anal.* Calc. for $C_{21}H_{17}AuCl_3N_3$: C, 41.03; H, 2.79; N, 6.84. Found: C, 40.40; H, 2.61; N, 6.42%.

*4.5.3. Synthesis of dichloro[2-(3,5-di-tert-butylpyrazol-1-ylmethyl)pyridine]gold(III) chloride (**7**)*

Compound **7** was prepared from **L3** (0.09 g, 0.32 mmol) and $H[AuCl_4] \cdot 4H_2O$ (0.13 g, 0.32 mmol). The product was obtained as a yellow powder after recrystallization from dichloromethane and hexane. Yield = 0.11 g, 60%. ^{1}H NMR (300 MHz, CD_3CN, 25 °C): δ 8.97 (d, $^3J_{H,H}$ = 5.70 Hz, 1H, py), 8.10 (t, $^3J_{H,H}$ = 7.80 Hz, 1H, py), 7.70 (t, $^3J_{H,H}$ = 6.90 Hz, 1H, py), 6.48 (d, $^3J_{H,H}$ = 7.80 Hz, 1H, py), 6.16 (s, 1H, pz), 5.96 (s, 2H, –CH_2), 1.58 (s, 9H, *t*Bu), 1.45 (s, 9H, *t*Bu). ^{13}C{^{1}H} NMR (75 MHz, CD_3CN, 25 °C): δ 159.0 (C2-Py), 154.3 (C3-pz),150.6 (C6-py), 144.8 (C5-pz), 128.4 (C3-py), 128.1 (C5-py), 102.6 (C4-pz), 56.5 (–CH_2), 30.7 (*t*Bu), 30.4 (*t*Bu). *Anal.* Calc. for $C_{17}H_{25}AuCl_3N_3$: C, 35.53; H, 4.38; N, 7.31. Found: C, 35.13; H, 3.93; N, 6.91%.

*4.5.4. Synthesis of dichloro[2-(3-para-tolylpyrazol-1-ylmethyl)pyridine]gold(III) tetrachloro-aurate (**8**)*

Compound **8** was prepared from **L4** (0.12 g, 0.48 mmol) and $H[AuCl_4] \cdot 4H_2O$ (0.12 g, 0.48 mmol). The product was obtained as a red solid. Yield = 0.17 g, 42%. Red crystals of **9** suitable for X-ray structure determination were obtained by slow evaporation of acetonitrile solution at room temperature. ^{1}H NMR (CD_3CN): δ 7.80 (d, 1H, pz, $^3J_{H,H}$ = 2.40 Hz), 7.78 (s, 1H, py), 7.73 (s, 1H, py), 7.27 (s, 2H, Ph), 7.25 (s, 2H, Ph), 6.76 (d, 1H, pz, $^3J_{H,H}$ = 2.40 Hz), 5.74 (s, 2H, –CH_2), 2.36 (s, 3H, ptol). ^{13}C{^{1}H} NMR (75 MHz, CD_3CN, 25): δ 149.1 (2-py), 142.7 (C3-pz), 139.3 (6-py), 134.6 (*p*tol-*para*), 131.2 (4-py), 131.2 (C1-*p*tol), 130.4 (C5-pz), 129.2 (*p*tol-*meta*), 128.1

(*p*tol-*ortho*), 127.7 (3-py), 126.7 (5-Py), 104.8 (C4-pz), 52.5 (–CH_2), 21.3 (Me-ptol) ppm. *Anal.* Calc. for $C_{16}H_{15}Au_2Cl_6N_3$: C, 22.45, H, 1.77; N, 4.91. Found: C, 23.10; H, 1.75; N, 4.84%.

4.5.5. Synthesis of trichloro[4-(3,5-dimethylpyrazol-1-ylmethyl)pyridine]gold(III) (**9**)

To a solution of **L5** (0.03 g, 0.17 mmol) in ethanol (2 mL) was added dropwise a solution of $H[AuCl_4] \cdot 4H_2O$ (0.07 g, 0.17 mmol) also dissolved in ethanol (2 mL). A precipitate formed within 3 min. The yellow precipitate was filtered, washed with water followed by ether, and then dried under vacuum. Yield = 0.06 g, 72%. ^{1}H NMR (300, $CDCl_3$, 25 °C): δ 8.81 (d, $^3J_{H,H}$ = 6.30 Hz, 2H, py) 7.90 (d, $^3J_{H,H}$ = 6.30 Hz, 2H, py), 5.94 (s, 1H, pz), 5.34 (–CH_2). *Anal.* Calc. for $C_{11}H_{13}AuCl_3N_3$: C, 26.93; H, 2.67; N, 8.57. Found: C, 26.60; H, 2.60; N, 8.00%.

4.5.6. Synthesis of trichloro[4-(3,5-diphenylpyrazol-1-ylmethyl)pyridine]gold(III) (**10**)

Compound **10** was prepared from **L6** (0.05 g, 0.17 mmol) and $H[AuCl_4] \cdot 4H_2O$ (0.07 g, 0.17 mmol). The product was precipitated by addition of small amounts of water. Product was obtained as yellow solid. Yellow crystals of **10** suitable for X-ray structure determination were obtained by slow evaporation of acetonitrile solution at room temperature. Yield = 0.07 g, 64%. ^{1}H NMR (300 MHz, CD_3CN, 25 °C): δ 8.57 (d, $^3J_{H,H}$ = 6.60 Hz, 2H, py), 7.88 (d, $^3J_{H,H}$ = 6.60 Hz, 2H, py), 7.61 (d, $^3J_{H,H}$ = 6.60 Hz, 2H, Ph-pz), 7.45 (m, 8H, Ph-pz), 6.91 (s, 1H, pz), 5.67 (s, 2H, –CH_2). ^{13}C{^{1}H} NMR (75 MHz, CD_3CN, 25 °C): δ 147.6 (C_4-py), 143.2 ($C_{2,6}$-py), 134.0 ($C_{3,5}$-py), 130.3 (Ph), 130.1 (Ph), 130.0 (Ph), 129.9 (Ph), 129.8 (Ph), 129.2 (Ph), 129.1 (Ph), 126.5 (Ph), 126.4 (Ph), 105.3 (C_4-pz), 53.2 (–CH_2) ppm. *Anal.* Calc. for $C_{21}H_{17}AuCl_3N_3$: C, 41.03; H, 2.79; N, 6.84. Found: C, 41.64; H, 2.78; N, 6.77%.

4.5.7. X-ray structural determination

Crystal evaluation and data collection were performed on a Bruker CCD-1000 diffractometer with Mo Kα (λ = 0.71073 Å) radiation and the diffractometer to crystal distance of 4.9 cm. The initial cell constants were obtained from three series of scans at different starting angles. The reflections were successfully indexed by an automated indexing routine built in the SMART program. These highly redundant data sets were corrected for Lorentz and polarization effects. The absorption correction was based on fitting a function to the empirical transmission surface as sampled by multiple equivalent measurements [48]. A successful solution by the direct methods provided most non-hydrogen atoms from the *E*-map. The remaining non-hydrogen atoms were located in an alternating series of least-squares cycles and difference Fourier maps. All non-hydrogen atoms were refined with anisotropic displacement coefficients. All hydrogen atoms were included in the structure factor calculation at idealized positions and were allowed to ride on the neighboring atoms with relative isotropic displacement coefficients.

4.5.8. Biological activity

Eagle's medium with 0.1 mM non-essential amino acids was prepared by adding 2 mM L-glutamine, 1.0 mM sodium pyruvate and 5% bovine fetal calf serum. HeLa cells and human lymphocytes (PBMCs) from preservative free heparinized peripheral blood were obtained from the Department of Pharmacology and Pretoria Medical Hospital, University of Pretoria, South Africa. The absorbance values were recorded on a Whittaker Microplate Reader 2001 spectrophotometer at 570 nm and the reference wavelength of 630 nm.

Cytotoxicity was determined by using the microtitration MTT assay after 7 days (3 days in the case of lymphocytes), which is reduced by living cells to yield a soluble formazan product that can be assayed colorimetrically [49]. A 20 μL volume of freshly prepared MTT (5 mg/mL) was added to each well and the cells incubated for another 4 h. Cell survival was evaluated by measuring absorbance at 570 nm, using a Whittaker Microplate Reader 2001. The IC_{50} values were calculated with the GRAPHPAD programme. All experiments were performed in triplicates.

Acknowledgements

We gratefully acknowledge financial support for this work from Project AuTek (Mintek and Harmony gold, South Africa) and the University of Johannesburg. We also wish to thank the Pharmacology department at the University of Pretoria for screening our compounds for their anticancer activity.

Appendix A. Supplementary material

CCDC 697852, 697857, 697856, 697858, 697855, 697853 and 697854 contain the supplementary crystallographic data for **L6**, **2**, **2** · **NCMe**, **3**, **3a**, **8** and **10**. These data can be obtained free of charge from The Cambridge Crystallographic Data Centre via www.ccdc.cam.ac.uk/data_request/cif. Supplementary data associated with this article can be found, in the online version, at doi:10.1016/j.ica.2009.02.046.

References

[1] K.R. Barnes, S.J. Lippard, Met. Ions Biol. Syst. 42 (2004) 143.
[2] M. Fox, J.J. Roberts, Cancer Metast. Rev. 6 (1987) 261.
[3] C. Meijer, N.H. Mulder, H. Timmer-Bosscha, W.J. Sluiter, G.J. Meersma, E.G. de Vries, Cancer Res. 52 (1992) 6885.
[4] E. Fokkema, H.J. Groen, M.N. Helder, E.G. de Vries, C. Meijer, Biochem. Pharmacol. 63 (2002) 1989.
[5] B. Lippert, in: Cisplat: Chemistry and Biochemistry of a Leading Anticancer Drug, Wiley-VCH, Zürich, Switzerland, 1999.
[6] W. Dempke, W. Voigt, A. Grothey, B.T. Hill, H.J. Schmoll, Anti-Cancer Drug. 11 (2000) 225.
[7] D.C. Dobyan, J. Levi, C. Jacobs, J. Pharmacol. Exp. Ther. 213 (1980) 551.
[8] D.L. Bodenner, P.C. Dedon, P.C. Keng, R. Borch, Cancer Res. 46 (1986) 2745.
[9] M. van Beusichem, N. Farrell, Inorg. Chem. 31 (1992) 634.
[10] M. Cusumano, M.L. Di Pietro, A. Giannetto, J. Chem. Soc., Chem. Commun. 5 (1996) 2527.
[11] J. Holford, F. Raynaud, B.A. Murrer, K. Grimaldi, J.A. Hartley, M. Abrams, L.R. Kelland, Anti-Cancer Drug Des. 13 (1998) 1.
[12] M. Hay, Curr. Opin. Oncol. Endocr. Metab. Invest. Drugs 1 (1999) 319.
[13] (a) P. Köpf-Maier, H. Köpf, Chem. Rev. 87 (1987) 1137;
(b) M.J. Clarke, F. Zhu, D.R. Frasca, Chem. Rev. 99 (1999) 2511;
(c) M.D. Hall, R.C. Dolman, T.W. Hambley, in: A. Sigel, H. Sigel (Eds.), Metal Ions in Biological Systems, vol. 42, Dekker, New York, 2004, p. 297;
(d) K.R. Barnes, S.J. Lippard, in: A. Sigel, H. Sigel (Eds.), Metal Ions in Biological Systems, vol. 42, Dekker, New York, 2004, p. 143.
[14] L. Giovagnini, L. Ronconi, D. Aldinucci, D. Lorenzon, S. Sitran, D. Fregona, J. Med. Chem. 48 (2005) 1588.
[15] A. Casini, M.A. Cinellu, G. Minghetti, C. Gabbiani, M. Coronnello, E. Mini, L. Messori, J. Med. Chem. 49 (2006) 5524.
[16] D. Aldinucci, D. Lorenzon, L. Stefani, L. Giovagnini, A. Colombatti, D. Fregona, Anti-Cancer Drug. 18 (2007) 323.
[17] L. Messori, F. Abbate, G. Marcon, P. Orioli, M. Fontani, E. Mini, T. Mazzei, S. Carotti, T. O'Connell, P. Zanello, J. Med. Chem. 43 (2000) 3541.
[18] M. Coronnello, G. Marcon, S. Carotti, B. Caciagli, E. Mini, T. Mazzei, P. Orioli, L. Messori, Oncol. Res. 12 (2001) 361.
[19] L. Ronconi, L. Giovagnini, C. Marzano, F. Bettio, R. Graziani, G. Pilloni, D. Fregona, Inorg. Chem. 44 (2005) 1867.
[20] L. Ronconi, C. Marzano, P. Zanello, M. Corsini, G. Miolo, C. Maccà, A. Trevisan, D. Fregona, J. Med. Chem. 49 (2006) 1648.
[21] G. Marcon, S. Carotti, M. Coronnello, L. Messori, E. Mini, P. Orioli, T. Mazzei, M.A. Cinellu, G. Minghetti, J. Med. Chem. 45 (2002) 1672.
[22] F. Abbate, P. Orioli, B. Bruni, G. Marcon, L. Messori, Inorg. Chim. Acta 311 (2000) 1.
[23] T. Yang, J.Y. Zhang, C. Tu, J. Lin, Q. Liu, Z.J. Guo, Chin. J. Inorg. Chem. 19 (2003) 45.
[24] (a) U. Kalinowska, K. Matlawska, L. Checinska, M. Domagala, R. Kontek, R. Osiecka, J. Ochocki, J. Inorg. Biochem. 99 (2005) 2024;
(b) E. Ciesielska, A. Szulawska, K. Studzian, J. Ochocki, K. Malinowska, K. Kik, L. Szmigiero, J. Inorg. Biochem. 100 (2006) 1579.
[25] J. Kasparkova, V. Marini, Y. Najajreh, D. Gibson, V. Brabec, Biochem. 42 (2003) 6321.
[26] (a) G.B. Caygill, P.J. Steel, J. Organomet. Chem. 395 (1990) 375;
(b) R. Gupta, R. Mukherjee, Polyhedron 20 (2001) 2545.

[27] Y. Suzaki, T. Yagyu, Y. Yamamura, A. Mori, K. Osakada, Organometallics 21 (2002) 5254.
[28] L.R. Falvello, R. Garde, E.M. Miqueleiz, M. Tomás, E.P. Uriolabeitia, Inorg. Chim. Acta 264 (1997) 297.
[29] R. Bertani, C.B. Castellani, B. Crociani, J. Organomet. Chem. 269 (1984) C15.
[30] K. Suzuki, H. Yamamoto, Inorg. Chim. Acta 208 (1993) 225.
[31] J. Vicente, J.A. Abad, M.T. Chicote, M-D. Abrisqueta, J.-A. Lorca, M.C.R. de Arellano, Organometallics 17 (1998) 1564.
[32] M.E. Kastner, W.R. Scheidt, J. Organomet. Chem. 157 (1978) 109.
[33] J.A. Potenza, L. Zyontz, J. San Fillipo Jr, R.A. Lalancette, Acta Crystallogr., Sect. B 34 (1978) 2624.
[34] J. Vicente, M.D. Bermúdez, M.P. Carrillo, P.G. Jones, J. Organomet. Chem. 456 (1993) 305.
[35] I.A. Guzei, M. Wendt, Dalton Trans. (2006) 3991.
[36] R. Dorta, E.D. Stevens, N.M. Scott, C. Costabile, L. Cavallo, C.D. Hoff, S.P. Nolan, J. Am. Chem. Soc. 127 (2005) 2485.
[37] I.A. Guzei, SOLID-G Ver. 2.4, Computer Program for Characterization of Ligand Steric Behavior in Organometallic Compounds, 2008.
[38] P. Shi, Q. Jiang, J. Lin, Y. Zhao, L. Lin, Z. Guo, J. Inorg. Biochem. 100 (2006) 939.
[39] S. Schouteeten, O.R. Allen, A.D. Haley, G.L. Ong, G.D. Jones, D.A. Vicic, J. Organomet. Chem. 691 (2006) 4975.
[40] A.J. Canty, C.V. Lee, Organometallics 1 (1982) 1063.
[41] V. Ferretti, P. Gilli, V. Bertolasi, G. Marangoni, B. Pitteri, G. Chessa, Acta Crystallogr. C 48 (1992) 814.
[42] K. Ortner, U. Abram, Inorg. Chem. Commun. 1 (1998) 251.
[43] V. Bertolasi, G. Annibale, G. Marangoni, G. Paolucci, B. Pitteri, J. Coord. Chem. 56 (2003) 397.
[44] A.G. Orpen, M.J. Quayle, J. Chem. Soc., Dalton Trans. (2001) 1601.
[45] F.K. Keter, S.O. Ojwach, O.A. Oyetunji, I.A. Guzei, J. Darkwa, Inorg. Chim. Acta 694 (2009) 1393.
[46] N. Kitajima, K. Fujisawa, C. Fujimoto, Y. Morooka, S. Hashimoto, T. Kitagawa, K. Toriumi, K. Tatsumi, A. Nakamura, J. Am. Chem. Soc. 114 (1992) 1277.
[47] J. Elguero, E.G.R. Jacquier, Bull. Soc. Chim. Fr 2 (1968) 707.
[48] Bruker-AXS, SADABS V.2.05, SAINT V.6.22, SHELXTL V.6.10 and SMART 5.622 Software Reference Manuals, Bruker-AXS, Madison, Wisconsin, USA, 2000–2003.
[49] T. Mosmann, J. Immunol. Meth. 65 (1983) 55.